The effects of initial wedge taper on area-balancing restoration of a fold-thrust belt

Xiaodong Yang[1,*,#], David J. Sanderson[1], Lisa C. McNeill[1], Frank J. Peel[2]

[1] Ocean and Earth Science, National Oceanography Centre Southampton, University of Southampton, Southampton, SO14 3ZH, UK.

[2] Applied Geodynamic Laboratory, Bureau of Economic Geology, The University of Texas at Austin, Austin, TX, USA.

*Corresponding author, email: xdyang@scsio.ac.cn

now at Key Laboratory of Ocean and Marginal Sea Geology, South China Sea Institute of Oceanology, Chinese Academy of Sciences, Guangzhou 510301, China

Abstract

Conventional area balancing method uses a single regional slope, usually parallel to basal detachment and generally horizontal, to restore a deformed geological section to an initial rectangular shape. However, most fold-thrust belts exhibit a wedge or trapezium (i.e., a quadrilateral with at least one pair of parallel sides) shape in cross-section with stratigraphic sequence thinning into basin. Two new, simple, quantitative solutions are developed to restore a thrust belt with more realistic geometries, which assume that the initial shape is a trapezium. This allows exploration of the role of initial wedge taper (represented by surface slope and basal dip) in controlling shortening estimate using area-balancing. The new methods are tested against sandbox models and natural examples of fold-thrust belt using a range of input parameters to evaluate the uncertainties in shortening calculation. We find the results are very sensitive to both initial surface slope and initial basal slope. This study highlights the significance of initial wedge taper in determining shortening across a fold-thrust belt, with accurate shortening estimates requiring independent constraint of this important geometry. Previous studies that used area balancing to predict depth to

detachment and/or to estimate shortening without taking into account the effects of initial wedge taper may need re-evaluation.

Key words: structural restoration, area balancing, fold-thrust belt, regional slope, tectonic shortening

1. Introduction

Structural restoration is a technique that is applied to restore a strained geological cross-section to its original, undeformed state, and is an important part of making a structural interpretation (Fossen, 2016). It is basically a tool used to reconstruct unknown initial geometry of a cross-section from its imaged or interpreted final geometry (Fig. 1). Hence, it is concerned mainly with three elements:

(1) The <u>initial geometry</u>, i.e., the original shape of cross-section before deformation, which is usually unknown but may be constrained by pre-deformational history or setting (Fig. 1b);

(2) The <u>final geometry</u>, which is generally known to some degree of accuracy and resolution from surface and/or sub-surface data and analysis (Fig. 1a), note large uncertainties may exist as to subsurface geometries due to various structural interpretation strategy, data quality, model selection (e.g., Bond, 2015; Butler et al., 2018);

(3) The <u>kinematics</u>, i.e., the proposed movement path from initial geometry to final geometry, which generally involves assumption of various stages of tectonic deformation.

To perform a structural restoration, some form of balancing is employed as a fundamental principle (e.g., Chamberlin, 1910; Dahlstrom, 1969). This involves relating a geometrical measure in the deformed state to that in the undeformed state, such as length, area or volume, which is generally assumed to remain unchanged (balanced). Line-length balancing presumes constant bed length both in deformed and undeformed states, area balancing assumes that plane strain (i.e., layer-parallel strain and layer-perpendicular thickening) is operating during deformation to conserve cross-sectional area (e.g., Chamberlin, 1910;

Goguel, 1962; Dahlstrom, 1969; Hossack, 1979; Woodward et al., 1990; Allmendinger and Judge, 2013; Butler, 2013; Groshong, 2019), volume balancing postulates that rock volume remains constant during deformation (e.g., Yin and Groshong, 2006)

Chamberlin (1910) first used balanced cross-sections to calculate depth to detachment beneath a fold. Dahlstrom (1969) applied 2D balanced section construction to make predictions of subsurface trap geometry in the Foothills of the Canadian Rocky Mountains. Section balancing and restoration techniques are also used to estimate orogenic shortening (Hossack, 1979; Boyer and Elliott, 1982; Mitra and Namson, 1989; McQuarrie, 2004; Judge and Allmendinger, 2011; Masini et al., 2011), to validate structural interpretations and suggest need for revisions (Bally et al., 1966; Dahlstrom, 1969; Boyer and Elliott, 1982; Dahlstrom, 1990; Woodward et al., 1990; Wilkerson and Dicken, 2001), to indicate presence of significant layer-parallel strain (Koyi et al., 2004; Lathrop and Burberry, 2017), and to evaluate lateral compaction (Butler and Paton, 2010). Finally, sequential (or progressive) restoration using line-length balancing is occasionally applied to constrain fault order and infer deformation history (e.g., Yin and Kelty, 1991; Lickorish and Ford, 1998; Ghisetti et al., 2016).

Existing area balancing methods generally restore a section to a rectangle or parallelogram, with the upper boundary (i.e., surface slope) being horizontal and/or parallel to the detachment (Fig. 2a), i.e., assumption of constant layer thickness. However, changing layer thickness across thrust belts has been recognized in different tectonic settings mostly with sedimentary sequence thinning into basin, e.g., the northwestern Alps (Beck et al., 1998), Hikurangi accretionary prism (Ghisetti et al., 2016), and North American Cordillera (Allmendinger and Judge, 2013). Although the initial geometry is difficult to determine in such settings, it is unlikely to be a simple rectangle, questioning the validity of many existing restorations. McQuarrie (2002) accounted for basin-related changes in layer thickness to construct orogen-scale cross-sections based on stratigraphic sections and geological mapping in the central Andes. Previous studies have also addressed area balancing relations with initial wedge shape and thickness variations. Judge and Allmendinger (2011) presented a method to estimate shortening using area balancing between deformed-state polygons (based on cross sections) and an initial trapezoidal prism, and evaluate uncertainties in shortening estimate, Allmendinger and Judge (2013) explored area-balance relations for more complex initial prisms with non-uniform taper, suggesting that the uncertainty in thickness and shape of the initial stratigraphic wedge accounts for 60-70 % of total shortening error.

These pioneering works lay the foundation for further investigation into the role of more specific, often simplified or fixed, parameters of initial wedge shape (e.g., surface slope, basal dip) in area-balancing. In Euclidean geometry, a convex quadrilateral with a least one pair of parallel sides is referred to as trapezium in British English and as trapezoid in American English. Here we generalize the initial geometry of a stratigraphic wedge to that of a trapezium, thus allowing us to explore the effects of changing dip of the regional (surface) and basal slope on estimates of shortening using area balancing. We a) develop two new approaches to area balancing that take into account different regional slope and basal dip, b) test these methods against analogue model and natural examples, and c) discuss the uncertainties, limitions, applications and implications of the new approaches.

2. Background

2.1. The Chamberlin method

The notion of a balanced cross-section was introduced by Chamberlin (1910) to predict depth to detachment across a fold belt from detailed surface observations. This method provides the conceptual background for the use of models to predict structural geometries (e.g., Bucher, 1933; Goguel, 1962; Dahlstrom, 1969; Ramsay and Huber, 1987; Bulnes and Poblet, 1999; Butler, 2013). The Chamberlin (1910) method was originally developed for sedimentary sequences with initially parallel layers and a planar basal detachment, i.e., constant bed length and thickness (Fig. 2a). It uses the geometry of a folded layer to predict the detachment location underlying a fold. The regional is defined as the original position of this folded layer prior to deformation, and the excess area E_1 is the area of material in the fold that is uplifted by deformation to a position above this original. The two vertical pin lines Pin 1 and Pin 2 set up the boundaries of the strained section that is subjected to area balancing restoration.

The Chamberlin (1910) method involves three geometric parameters, obtained from the deformed cross-section: the length of folded layer L_0^*, the excess area above regional slope E_1 and the length L_1 between the two pin lines (Fig. 2a). Based on the assumption of line balancing and area balancing

$$L_0^* = L_0 \tag{1}$$

$$E_1 = E_2 \tag{2}$$

where L_0 is the original bed length equivalent to the length of undeformed cross-section, and E_2 is the area displaced above the detachment (Fig. 2a)

The shortening S is derived from bed length measurement by

$$S = L_0^* - L_1 \tag{3}$$

and the displaced area E_2 is determined by

$$E_2 = h * S = E_1 \tag{4}$$

where h is the depth to detachment. Note it is constant at the two pin lines because the regional and basal detachment are parallel in this model.

Rearranging formula (4) and substituting (3) gives the detachment depth

$$h = E_1 / S = E_1 / (L_0^* - L_1) \qquad (5)$$

The Chamberlin (1910) method can be reversed to calculate orogenic shortening of a cross-section if the depth to detachment is known (Hossack, 1979; Woodward et al., 1990; Moretti and Callot, 2012).

$$S = E_1 / h \qquad (6)$$

By using a single regional slope that is parallel to basal detachment, the Chamberlin (1910) method restores a geological cross-section to a rectangle, representing the initial geometry (Fig. 2a).

2.2. Limitations and need for modification

Despite significant progress in predicting subsurface geometry and shortening estimate by the Chamberlin (1910) method, several problems arise from the underlying assumptions:

(1) Bed length may not remain constant due to layer-parallel strain, with the shortening calculated using equation 3 being insufficient to account for the overall shortening of a cross-section. The predicted depth to detachment (equation 5) would then be substantially deeper than imaged (Faill and Nickelsen, 1999). This discrepancy is primarily caused by ignoring the penetrative layer-parallel strain, and has been recognized both in scaled physical models and field observations (Sans et al., 2003; Koyi et al., 2004; Butler and Paton, 2010; Groshong et al., 2012; Moretti and Callot, 2012; Wiltschko and Groshong, 2012; Şengör and Bozkurt, 2013; Lathrop and Burberry, 2017; Groshong, 2019).

(2) The Chamberlin (1910) method produces a rectangle or parallelogram for a restored cross-section with upper surface defining a ‘regional slope’ that is parallel to a planar, usually horizontal, basal detachment (e.g., Dahlstrom, 1969; Hossack, 1979; Mitra and Namson, 1989; Moretti et al., 2006; Moretti et al., 2007; Butler, 2013; Schori et al., 2015;

Hubbard et al., 2016). In fact, this is not the case for most fold-thrust belts and accretionary prisms, where the basal detachment is typically dipping to the hinterland (Davis et al., 1983; Dahlen, 1990) (Fig. 2b). If the regional slope remains horizontal, the restored cross-section is therefore a right trapezium, a trapezium that has at least two right angles, rather than a rectangle (Fig. 2b). This right trapezium is composed of two parallel sides (vertical in this case) equivalent to the boundaries of a retro-deformational cross-section, a horizontal line representing the regional slope and an oblique line representing the inclined detachment. Previous studies incorporated changes in stratigraphic thickness into constructing and restoring cross-section (e.g., McQuarrie, 2002; Judge and Allmendinger, 2011) found that the initial wedge taper is of great importance to area-balancing. A quantitative investigation into the role of most important parameters of wedge taper (i.e., regional slope, basal dip) in area-balancing is required.

(3) In many geological settings, the initial regional slope of a stratigraphic layer needs not be horizontal (e.g., Mishra and Mukhopadhyay, 2012). Fold-thrust belts and accretionary prisms typically exhibit an overall wedge shape with a foreland-dipping topographic slope and a hinterland-dipping basal detachment, generally as a result of both tectonic deformation (i.e., shortening and thickening, Davis et al., 1983) and pre-deformation deposition of sediments (i.e., thinning layer thickness towards foreland; Beck et al., 1998; Ghisetti et al., 2016; Wang et al., 2018). This suggests that both initial regional slope and basal slope of a thrust wedge are probably not horizontal and parallel, but form as a wedge (Fig. 2c), although they may be difficult or impossible to reconstruct. In this paper we explore the idea of restoring cross-sections to a general trapezium of any initial regional and basal slope, including right trapezium (Fig. 2b,c).

3. Methodology

We represent undeformed section as a general trapezium (blue in Fig. 3) that is pinned on the left. The trapezium sits on a presumed single detachment that marks the base of the cross-section and dips to hinterland (i.e., basal slope = β), and has a surface slope α_0. Surface slope (α_0) is assumed to be built entirely by structural deformation of stratigraphic sequence (i.e., thrusting, folding, Figs. 3 and 4), which is not exactly same as present-day topographic relief, because the latter may reflect, to some extent, both tectonic deformation and surface process (including post-kinematic deposition). It is defined here that an increase in basal slope leads to steepening detachment towards hinterland while an increase in surface slope results in steepening topography towards foreland (Fig. 3). We note that the basal slope may change during deformation from flexural loading (e.g., Boyer, 1995; Mitra, 1997), but it is difficult to quantify.

For the purpose of simple area-balancing restoration, we assume the basal dip to remain constant throughout time, similar to the model setting of many scaled analogue experimentation of thrust wedge (Wu and McClay, 2011; Schreurs et al., 2016). First, we consider moving a rigid, right-hand region from right to left, assuming it acts as a vertically continuous 'end-plate', similar to the 'snow-plough' envisaged in the critical taper theory (Davis et al., 1983). If the trapezium deforms homogeneously it will produce a new trapezium with greater surface slope α that resembles the resultant shape of fold belt (Fig. 3). Note that the surface slope α generalizes the first-order topographic relief of a thrust belt in line with the critical taper theory of Davis et al. (1983). The excess area (E_1) above the regional is balanced by a trapezium of equal area (E_2) to the right of the 'end-plate' (Fig. 3), which is equivalent to 'back-stop' used in many critical taper models. Model 1 represents a special case of the polygon area-balance model of Judge and Allmendinger (2011), i.e., a simply deformed polygon with four vertices.

An alternative model (Model 2) assumes that the material to the right (hinterland) simply moves up along basal detachment with no internal deformation, and that there is strain continuity between this and the deforming wedge (Fig. 4). This situation is approximated in many fold-thrust belts and will produce heterogeneous deformation in wedge and produce an excess area A_E above the pseudoregional slope that connects the top corners of the deformed wedge (OB in Fig. 4) and links the stratigraphy across the wedge. Note that this is not the true regional as the right-hand region has been displaced up the detachment. Model 2 has variable thickness in wedge, with thickening diminishing to 0 at both ends. It corresponds to the polygon model of Judge and Allmendinger (2011) in which the depth from the vertices on prism sides to the basal detachment do not change.

3.1. Model 1, trapezium shape

We assume that the original shape is a trapezium, with surface slope α_0 and basal dip β (blue in Fig. 3). Shortened by a distance *S*, with the material deforming homogeneously, produces a trapezium with slope α (red in Fig. 3). The two vertical sides of the trapezium remain parallel. The front one is a fixed boundary (i.e., in x, y direction) and has no height change (i.e., h_0), whereas the 'back one' moves forward and allows slip parallel to it, thus the thickness within the sediments pile changes from h_2 to h_1 (Fig. 3). This is similar to the setup of scaled sandbox models with a fixed wall in the front and a mobile wall in the back (e.g., Schreurs et al., 2006). In this model, the parameters that are essential to area-balancing restoration are dip of basal detachment (β), length of section (L_1) and depth to detachment at the deformation front (h_0) and at the backstop (h_1). From these we can determine the final slope angle (α) and cross-sectional area *A*.

$$A = L_1 [½ L_1 \tan \alpha + ½ L_1 \tan \beta + h_0] \quad (7)$$

Two model parameters, basal dip (β) and depth to detachment (h_0) at wedge front, are fixed during restoration. Generally, we only need to assume a value for the original topographic slope (α_0) in order to determine the excess area (E_1) and, thus, the restored shortening of cross-section (Fig. 3). However, instead of using excess area to restore a cross-section, as adopted in conventional area balancing method (Chamberlin, 1910; Dahlstrom, 1969; Hossack, 1979), we use the area of trapezium as a whole to restore the section based on area preservation. Under these conditions, the assumed initial regional slope α_0 is utilized, in combination with the shortening S, to obtain the cross-sectional area A of the restored section (i.e., blue trapezium in Fig. 3), where

$$A = (L_1 + S)\ [\ \tfrac{1}{2}\ (L_1 + S) \tan \alpha_0 + \tfrac{1}{2}\ (L_1 + S) \tan \beta + h_0] \qquad (8)$$

Although the final area of a fold-thrust belt has uncertainties related to detachment depth and erosion of material, based on the assumption of conserved area, the restored cross section area A is considered to be equivalent to the deformed cross-section area, which is a known parameter (Fig. 3). The initial length of section L_0 is the sum of current wedge length and restored shortening ($L_0 = L_1 + S$) and substituting in (8) gives:

$$A = L_0\ [\tfrac{1}{2}\ L_0 (\tan \alpha_0 + \tan \beta) + h_0] \qquad (9)$$

Equation (9) is a quadratic equation with one unknown L_0, and can be rearranged as:

$$\tfrac{1}{2}\ (\tan \alpha_0 + \tan \beta)*(L_0^2) + h_0*(L_0) - A = 0 \qquad (10)$$

the solution for the original wedge length L_0 and, hence, shortening ($S = L_0 - L_1$)

$$S = \frac{-h_0 + \sqrt{h_0^2 + 2A\ (\tan \alpha_0 + \tan \beta)}}{(\tan \alpha_0 + \tan \beta)} - L_1 \qquad (11)$$

Although the excess area E_1 is not used in the restoration presented above, its value can be resolved by geometric analysis (Fig. 3). The difference between the known overall cross-sectional area A and the trapezium constrained by two pin lines, basal detachment and initial regional slope (Fig. 3)

$$E_1 = A - \frac{1}{2}(h_0 + h_1) L_1 \quad (12)$$

This method avoids one single regional scenario of restoring deformed section to a rectangle. Instead, the model uses a trapezium to provide a more general shape of initial wedge and restored thrust belt (Fig. 3). Figure 5 shows a sequence of developed thrust wedges (trapezium shape) for the initial wedge (pink) of length = 100 km, h_0 = 2.5 km, basal slope β = 2° and surface slope α_{01} = 1.1°, subjected to shortening of 10, 20 and 30 km in correspondence to the resulting yellow, green and red trapeziums. Note the surface slope (α) of the resulting trapeziums cannot exceed the maximum surface slope with constant basal dip (i.e., critical taper) as predicted by Davis et al. (1983). The sequence of thrust belt development predates attainment of a critical taper angle. If we consider the red trapezium as a strained cross-section, then the other trapeziums could be seen as various restored shapes assuming different initial regional slopes (α_{03}, α_{02}, α_{01}), which gives estimated shortening values S_{03}, S_{02} and S_{01}. These results are generalized in Fig. 5b and, clearly, the estimated shortening is very dependent on the assumed regional slope, with an increase in regional slope accompanied by a decrease in the predicted shortening (Fig. 5b).

3.2. Model 2, assuming continuity and using a pseudoregional slope

The model in the previous section is very simple and assumes a homogeneous strain in deformed wedge, with no deformation behind this, and with a discontinuity in strain at the "backstop". In most fold-thrust belts there is some degree of continuity between the deformed and undeformed regions. If we assume that the material to the right (hinterland) simply moves up basal detachment with no internal deformation and that the deformation in such fold-thrust belt is heterogeneous and simply dies out to the vertical walls of the trapezium, then we have a situation as in Figure 4. Continuity between the deformed and undeformed regions means that lengths $h_1 = h_2$, with the height of h_2 simply raising from A to B as the undeformed region slides up the basal detachment. The slope of OB is different from the true regional of OA (Fig. 4), and is defined here as the pseudoregional slope. In this case it is useful to consider this pseudoregional slope and determine the excess area above it (A_E) and the area of trapezium below it, $A_\#$ (constrained by OBB'O'):

$$A_\# = ½ (h_0 + h_2) L_1 \quad (13)$$

Balancing this area of the original trapezium gives :

$$A_0 = A_E + A_\# = A_E + ½ (h_0 + h_2) L_1 \quad (14)$$

Since:

$$A_E = A_0 - A_\# = ½ (h_0 + h_2) S \quad (15)$$

Which on rearranging gives:

$$S = 2 A_E / (h_0 + h_2) \quad (16)$$

Equation (16) allows shortening to be calculated directly from the area above the pseudoregional slope.

3.3. Model assumptions, uncertainties and limitations

Surface processes (i.e., erosion and sedimentation) also change topography (including surface slope α_0 in this case, Fig. 3) of a thrust wedge by addition or removal of material at surface, isostatic response to changes in overburden (i.e., flexural loading) (Beaumont et al., 1992; Storti and McClay, 1995; Willett, 1999; Hilley and Strecker, 2004; Hoth et al., 2007; Morley, 2007a; Cruz et al., 2010; Fillon et al., 2013). Erosion of pre-kinematic sequence reduces the resultant bed-length and cross-sectional area, causing an underestimate of shortening. In this study, we minimize the effect of erosion on area balancing by either not restoring the eroded area or restoring the eroded area after reconstructing it based on the underlying stratigraphic geometry. The method assumes plane strain with final cross-sectional area (i.e., red trapezium in Fig. 3) being equivalent to initial cross-sectional area (i.e., blue trapezium in Fig. 3).

The models assume a thrust wedge underlain by a single basal detachment (Figs. 3,4). Some real-world examples are found to have multiple detachments with various depth, (e.g., Niger Delta, Corredor et al., 2005), involving more complicated deformation in response to contraction. The single detachment approximation in this study (and most others) will inevitably ignore this complex deformation, leading to uncertainties in final shortening estimates.

The single basal detachment is also assumed to remain constant in dip during deformation, similar to the critical taper wedge model (Davis et al., 1983). However, in many orogenic belts, the dip may change in response to flexural loading (e.g., Boyer, 1995; Mitra, 1997), while in others, the basement may be deformed by deep-rooted thrusting, leading to more complex detachment geometries (e.g., McQuarrie, 2002; Butler et al., 2004; Molinaro et al., 2005). These aspects are not addressed here, and require further investigation.

In natural examples, the deformation front also propagates forward through frontal accretion with increasing contraction. The trapezium model presented here assumes that the position of deformation front is fixed (Figs. 3, 4), resembling the geometric settings of scaled numerical and physical analogue models (Buiter et al., 2016; Schreurs et al., 2016). Our area-balancing simply restores thrust wedge to its pre-deformed state using a range of initial surface slopes.

3.4. Comparison with other structural restoration techniques

Apart from area balancing, previous authors also applied progressive restoration method based upon bed-length measurement to reconstruct the tectonic history of a thrust belt and estimate associated shortening (e.g., McQuarrie, 2004; Corredor et al., 2005; Hesse et al., 2009; Hesse et al., 2010; Masini et al., 2011; Ghisetti et al., 2016). The estimated shortening by these techniques is typically cited as a minimum estimate (Allmendinger and Judge, 2013) as bed-length may not conserve during deformation (Epard and Groshong, 1995; Koyi et al., 2004; Butler and Paton, 2010; Groshong et al., 2012; Wiltschko and Groshong, 2012; Şengör and Bozkurt, 2013; Lathrop and Burberry, 2017). To avoid the restriction of bed-length change, the Area-depth-strain (ADS) method is proposed to predict the detachment depth, estimate shortening and detect sub-resolution deformation based on the relationship between excess area of multiple stratigraphic horizons on a cross section and their relative depths (Epard and Groshong, 1993; Groshong and Epard, 1994; Groshong et al., 2012; Wiltschko and Groshong, 2012; Schlische et al., 2014). This method is effective to calculate shortening since it is independent of bed-length, detachment depth and dip, and is insensitive to bed-length changes. However, the ADS method was initially proposed to deal with individual fault-related folds of conserved stratigraphic thickness, i.e., initially parallel (mostly horizontal) bedding and basal detachment. A real-world thrust belt is generally composed of a series of folds, oblique basal detachment with varying stratigraphic thickness that together make it challenging for ADS method to determine the initial regional slope for each stratigraphic layer, hence limiting the use of ADS method in system of this kind.

Our models require good constraints on final geometry of a thrust wedge, e.g., depth to detachment, basal dip, bounds on deformation. The results obtained from Model 1 allow us to examine the sensitivity of excess area and shortening to changes in regional surface slope (e.g. Fig. 5). Model 2 helps to compute an independent shortening but requires known initial depth to detachment prior to deformation (Fig. 4). Combination of Model 1 and 2 enables to constrain shortening result and its corresponding regional slope. These analysis highlight the uncertainties in the selection of regional slope, as such our methods can be complementary to the ADS method in determining an appropriate regional to optimize its application in a complicated fold-thrust belt.

Wang et al. (2018) present a method for improving the ADS graph so that it can be used to analyze wedged shaped strata of varying thickness, and a dipping, bed-parallel detachment. This improved ADS method is capable of estimating various depth and dip angle for an underlying oblique detachment, and it is independent of not only bed-length, but also bed-thickness and regional horizon throws. In Wang et al.'s (2018) analysis, one of the specific parameters they account for is regional dip on each bed used in area-depth-graph. The varying regional slope between different horizons is approximated by simply connecting the undeformed dipping bed from both sides of a fold or across a range of folds, which works well in a region where the deformation is localized in folds and the undeformed area shows apparently constant bed dip. However, in a region deformed by complex folds and thrusts with effects of flexural loading, the present-day stratigraphic sequence may show variations in dip across thrust wedge, making it difficult to approximate a regional slope across a fold or a series of folds. In our models, we show how significant the initial regional slope is to area-balancing. This is important because the improved ADS method for sedimentary wedges requires an estimate of regional slope for each horizon.

3.5 Comparison of Model 1 and Model 2

Model 1 highlights the significant role of surface slope (and basal dip) in area-balancing restoration, but its results for shortening do not converge (Fig. 5) because a range of initial surface slope is used in computation. Further, the precise initial surface slope of a thrust belt is generally unknown, which makes the Model 1 difficult to estimate shortening independently.

In contrast, Model 2 yields a unique shortening estimate by assuming a strain continuity between the deformed region and backstop. However, if the rear of wedge also experiences thickening, it may underestimate shortening (Fig. 4, equations 13-16). In real application, if the initial surface slope (and basal dip) is well constrained, Model 1 can be used to compute shortening of a thrust wedge with slightly more complex calculation process, whereas if the initial depth to detachment is known, one can approximate a pseudoregional slope by projecting the topography of stratigraphic sequence in front of the deforming wedge all the way to the rear of wedge, and apply Model 2 to calculate shortening with simple calculation process.

4. Application to fold-thrust belts

4.1. Scaled physical analogue models

To validate the models (Figs. 3 and 4), we used a scaled physical analogue example (Granado et al., 2017) where the initial geometry, final geometry and imposed shortening (Fig. 6a) are known. The example has an initial surface slope of 3° (α_0), length of 75 cm (L_0), detachment depth at the wedge front of 6 cm (H_0), and was subjected to 15 cm shortening, creating a fold-thrust belt (Fig. 6a). Two horizons with well-defined initial slopes are taken to perform the area balancing restoration using Model 1 (Fig. 3, red trapezium is the deformed wedge while the blue trapezium is the restored wedge): top layer with initial slope 3° (Fig. 6b) and base of yellow layer with initial slope 0° (Fig. 6a, Granado et al., 2017). This allows a direct comparison of restored shortening values for different dipping layers.

We first created a green trapezium with same cross-sectional area A, wedge length L_1, basal dip β and depth to detachment at front h_0, as the resulting thrust belt (brown and yellow wedge in Fig. 6b & 6c). The structural restoration with base of horizontal yellow layer (0° of initial slope) produced 14.8 cm shortening (Fig. 6c, Table 1), roughly consistent with the 15 cm applied in the experiment. This validates the calculated shortening based on restoration to a rectangle, i.e., Chamberlin (1910) method.

Figure 6b shows the restored section based on the top layer with an initial slope of 3° (blue trapezium), which yields 12.7 cm of shortening (Table 1), a little less than that applied 15 cm shortening (Granado et al., 2017). Using a 2.5° initial slope to restore the cross-section gives 14.7 cm of shortening, very close to the initial model setting. The 3° slope setting by the model is likely a first-order estimate and yields a shortening of 12.7 cm. The difference in shortening between the model (Granado et al., 2017) and results using Model 1 can be attributed to uncertainties in geometrical measurement, i.e., area, surface slope, h_0, layer parallel shortening (e.g., Koyi et al., 2004).

From the undeformed sand wedge, we know the initial height h_2 next to the mobile wall (Granado et al., 2017). If this height maintains its value and moves forward as the undeformed region slides along the basal detachment, we know that BB'= h_1=h_2, and thus we can estimate the pseudoregional slope OB (Fig. 7). We can then calculate the shortening using Model 2 (Fig. 4) and, from equation 16, we estimate 14.5 cm of shortening (Fig. 7, Table1), very close to the experiment value of 15 cm.

In addition to measurement uncertainties, the slight underestimates in the shortening may be due to tectonic compaction, layer-parallel shortening and lateral compaction (e.g., Koyi et al., 2004; Butler and Paton, 2010). But the overall good agreement between our area balancing restoration show that the proposed restoration models are able to estimate shortening based area balancing. Further application of the models to real-world examples are presented in the following sections.

4.2. Hikurangi accretionary prism, New Zealand

The Hikurangi accretionary wedge is generated by the subducting oceanic Pacific Plate along the eastern margin of North Island, New Zealand. Three depth-converted and geologically interpreted seismic profiles across the central Hikurangi margin were sequentially restored to study the last 2 Myr tectonic history of wedge development by Ghisetti et al. (2016). To test our theoretical model against natural examples, we took one of these cross-sections (transect T03 in Ghisetti et al. (2006), for location see the map of Fig. 8d) to carry out area balancing restoration using Model 1.

Fig. 8a shows that the accretionary prism is dominated by imbricated thrusts and related folds that all sole out into one single detachment. Six stratigraphic units are interpreted with inferred age of present day to 15±5 Ma, i.e., color grey to blue (Fig. 8a). The top orange layer (R3), with inferred age of 0.6±0.2 Ma, is used to define a wedge with 330.7 km^2 of cross-section area (A) and length (L_1) of 85.7 km, sitting above a detachment with a frontal depth (h_0) of 1.9 km (see also Table 1). We created a simplified trapezium model (black trapezium in Fig. 8b), to match in deformed wedge. A horizontal regional is assumed to restore the black trapezium to blue trapezium, yielding 8.2 km of shortening (Fig. 8b). We then tested a range of regional slopes from -0.3 to 0.6 ° using Model 1, which produced shortening results ranging between 0.4-13.5 km (Fig. 8c), with the estimated shortening being inversely correlated with dip of regional slope (as Fig. 5b).

Ghisetti et al. (2016) estimated 11.6 km of shortening accommodated during the deposition of R5-R3 by sequential restoration essentially based on bed length measurement and area balancing, which exceeds the 8.2 km of shortening across the thrust belt estimated using a horizontal regional (Fig. 8b). A few factors are thought to contribute to the difference. Firstly, the horizon R3 does not exclusively mark the top of pre-kinematic strata, at the landward area, it is actually preserved in a post-kinematic sequence (Fig. 8b). So the layer R3 does not record all the deformation, particular in the landward area of the thrust belt, and will be an underestimate of shortening. Secondly, some erosion is observed at the crest of a fold (Fig. 8a), which leads to the removal of part of Horizon R3 and underlying horizon R4, reducing the cross-sectional area and, hence, underestimating shortening. Thirdly, the assumption of 0° at minimum for regional slope might be wrong. Using Model 1, a landward dipping surface slope of – 0.2° would be necessary to produce the 11.6 km shortening estimated by Ghisetti et al. (2016). This is supported by the landward dip of horizon R6 in front of the fold-thrust belt (Fig. 8a).

We noted that this may be a less fair comparison between our model result and the result of Ghisetti et al. (2016) since horizon R3 is not entirely pre-kinematic, thus shortening is possibly underestimated in our methods. In addition, the initial wedge geometry is largely unknown, which leaves the results of both methods be difficult to validate. The objective of this example study and result comparison is to demonstrate the importance of regional slope in shortening estimate, without good constraint on such essential parameter, the shortening is highly variable. This will be further discussed in the Discussion (Mitigating issues with area balancing methods).

4.3. NW Borneo fold-thrust belt

The NW Borneo continental margin is well known from drilling and seismic reflection data related to hydrocarbon exploration (Inset in Fig. 9) (Hinz et al., 1989; Ingram et al., 2004; Morley et al., 2008; Hesse et al., 2009; Morley, 2009a; Hesse et al., 2010). The NW Borneo fold-thrust belt (FTB) is developed on the deep water slope in the middle Miocene-Holocene shallow marine sequences (Morley, 2009b). Previous 2D seismic data shows an extensive train of elongated folds that verge seaward, spaced 5-15 km apart and oriented NE-SW (Hinz and Schluter, 1985; Hinz et al., 1989; Morley, 2009a).

3D seismic datasets was acquired and processed by Petroleum Geo-Services (PGS) in 2000 and 2001, covering some 10,000 square kilometres of the deep-water area off Brunei (Morley, 2009a). Figure 9 shows interpreted seismic profiles A, B and C with five horizons being mapped from shallow to deep levels (H0-H4) within the pre-kinematic sedimentary sequence. Folds and associated imbricate thrusts that sole out at depth into one detachment, South China Sea Unconformity (SCSU) (Morley, 2009a), and form a trapezium geometry with topographic slope dipping to foreland and basal detachment dipping landward (Fig. 9). Area balancing was preformed between two pin lines shown in each example.

Horizon H0 is partly eroded at the crest of anticlines in profiles B and C, (see also Gee et al., 2007; Morley, 2007b; Morley, 2009b), and was reconstructed based upon the geometry of underlying sedimentary layer, i.e., H1 (Fig. 9). This inevitably leads to some inherent uncertainty in the structural interpretation. Due to the reduced seismic resolution at depth, lowest mapped horizon (H4) is also interpreted with less confidence. To minimize these uncertainties, we only use the most reliable seismic horizons H1-H3 to conduct the restoration. Horizon H1 is mapped as one of the top layers of pre-kinematic sediments, its geometry is thought to represent the overall topography of the deforming thrust belt.

4.3.1. Restorations based on Model 1 and Model 2

The thrust belt enveloped by horizon H1 is taken as an example for area balancing restoration using our Model 1 (Figs. 3 and 5, equation 7-12). We created simple trapezium models (red trapeziums in Fig. 10) to match the overall shape of the fold belt, with same cross-section area *A*, wedge length L_1, depth to detachment at the front h_0, and basal dip β

(Table 1). We then restored this, maintaining h_0 and β to the blue trapezium in Fig. 10 using an arbitrary horizontal regional, $\alpha_0 = 0°$, which yields 17.0, 13.6 and 8.3 km shortening for three examples from profiles A, B and C (Table 1). If a horizontal regional slope is the case across the study area, the calculated shortening shows a distinct decreasing trend from profile A to C, i.e., from southwest to northeast despite a significant difference in wedge parameters across these three sections, such as wedge length L_1, depth to detachment at front stop h_0, angle of basal dip β and area of cross-section A (Table 1).

We repeated the area balance using a range of initial regional dips from 0-1.5° for horizons H1-H3 (Fig. 11). These give a variety of shortening estimates ranging between 0-21.5 km, indicating that the shortening estimated by area balancing is highly sensitive to the select of regional dip. To better constrain the results, additional efforts are needed.

We then applied our Model 2 (Fig. 4) to estimate the shortening across the fold-thrust belts by measuring the area above the pseudoregional slope (A_E) and depth to detachment at the front (H_0) and backstop (H_1) (equation 13-16). The overall results of applying Model 2 to horizon H1 are presented in Table 1. As shown in Fig. 11, a narrow range of 4.5-4.8 km of shortening is quantified for each section, but the corresponding regional slope is determined to range from 0.7-1.3°.

Taken together, these models suggest: (1) using the same initial regional slope (0°) produces shortening estimates that range from 8.3-17.0 km in different sections (Model 1, Fig. 10); (2) these shortening estimates are very dependent on the value of regional slope used (Fig. 11); (3) application of model 2 produced similar shortening (~4.5-4.8 km) in all three sections, but only with the initial regional slopes varying from 0.7-1.3° in different sections (Fig. 11). In the next section we address, which, if any of these possible interpretations is plausible.

4.3.2. Comparison with studies in the adjacent region

Previous workers have investigated the along-strike shortening across other parts of the NW Borneo fold-thrust belt (e.g., Hesse et al., 2009; Totake et al., 2018). Totake et al.'s (2018) only documented the total shortening of 3 folds based on bed-length measurement in the fold thrust belt. The study of Hesse et al. (2009) estimated the shortening across the entire fold thrust belt and is closest to this study area, which is chosen to compare with our results and make evaluation on different interpretations described above. Hesse et al. (2009) estimated the 2.7-7.2 km of shortening across the Northern Brunei and Sabah portion of the NW Borneo FTB, some 50-300 km northeast of this study area, using progressive restoration based on bed-length measurement (Fig. 12). Within this range, 4-6 km of shortening is estimated across the Northern Brunei with a slight increase to the NE.

This contrasts significantly with our results derived by Model 1. As shown in Fig. 12, a horizontal regional slope gives 8.3-17 km of shortening while 0.6° regional slope produces 5.2-10.2 km of shortening. Both are much higher than that estimated by Hesse et al. (2009), and also show a prominent, opposite varying trend, i.e., increasing towards northeast. This suggests that the result derived from Model 1 are highly variable, and very sensitive to the select of initial regional slope. However, the result of Model 2 ranges narrowly between 4.5-4.8 km (Fig. 12), in general consistency with that quantified by Hesse et al. (2009). If the Brunei portion of NW Borneo FTB experiences similar amount of contraction in a narrow range of 4-6 km, the result of Model 2 appears to be more likely (Fig. 12).

We noted there is variability in shortening estimate, structures and lithology (e.g., Hesse et al., 2009; Totake et al., 2018) along strike between adjacent lines in this offshore area, but the overall trend of shortening gives us a first order control on the scale of deformation

(Fig. 12). The comparison analysis presented here is aimed to show a range of possible results that may arise from area balancing if there is no good control on initial surface slope.

5. Discussion

5.1. The role of basal dip

So far this study has only explored the role of regional (surface) slope with fixed basal dip in area-balancing restoration. Similarly, the dip of basal detachment also has significant effect on area-balancing method. Assuming a fixed surface slope (e.g., $\alpha_0 = 0$), an increase in basal dip (i.e., steepening towards hinterland) is accompanied by an overall increase in the thickness of initial wedge. Given the measured individual value of cross-sectional area of a deformed wedge, these changes will lead to lower estimates of shortening. So the surface slope and basal dip play a similar role in area-balancing restoration.

5.2. Mitigating issues with area balancing method

Previous studies have paid little attention to the effect of initial wedge taper in area balancing restoration (Chamberlin, 1910; Dahlstrom, 1969; Hossack, 1979; Mitra and Namson, 1989; Woodward et al., 1990; Groshong et al., 2012; Wiltschko and Groshong, 2012; Butler, 2013). The estimation of excess area using a simplified initial regional slope (Mitra and Namson, 1989; Wiltschko and Groshong, 2012; Schlische et al., 2014), implicit in most applications of area balancing restoration ignores the dependency on dip of the regional slope (as part of initial wedge taper). The traditional method is valid only if a geological cross-section is composed of layer-parallel sedimentary sequences above a single basal detachment (Chamberlin, 1910), which in fact does not reflect the complexity of structural features in natural thrust systems. Such features include: sedimentary wedges with stratigraphic sequence thinning towards the foreland and thickening towards the hinterland; multiple detachment levels; complex fault related folds; forward and backward vergent imbricate thrusts and duplexes (Boyer and Elliott, 1982; Davis et al., 1983; Dahlen, 1990; DeCelles et al., 1998; McQuarrie, 2004; Fitz-Diaz et al., 2011; Wang et al., 2018). Further, due to flexural loading and folding, the excess area above a simplified straight regional slope might be segmented (i.e., not all excess area above the regional slope), which leads to underestimate of excess area and thus shortening in previous area balancing.

To mitigate these issues, our Model 1 restores the entire strained cross-section (Fig. 5), rather than the excess area only by previous study (e.g., Chamberlin, 1910). This effectively avoids one single regional slope approximation and underestimation of excess area and shortening in case of flexural loading in traditional methods. The application of our methods to scaled physical analogue shows a good agreement between the theoretical predication and physical experiment (Figs. 6 and 7) owing to the known initial dimension of experiment model (Granado et al., 2017). However, the application of our methods to natural examples are not well constrained (Figs. 8 and 12) due to the unknown initial geometry for these examples, and which also makes it difficult to determine the correct answer derived from different strategies. However, these case studies highlight the critical role that the initial wedge geometry plays in estimating orogenic shortening across a geological cross-section. Without good control on initial wedge taper, the estimated shortening can be highly variable (Figs. 8&11).

5.3. Uncertainties of area balancing approach

Despite progress made by this study, any balancing method is still subjected to uncertainties in (A) the geometry of deformed area, (B) the assumed shape of restored area and (C) the validity of balancing conditions (conservation of length, area, etc).

Type A

Type A errors are based mainly on structural mapping and interpretation of the fold-thrust belt (including imaging and correlation of horizons, recognition of facies changes, erosion, etc.) and location of detachment (e.g., Bond, 2015; Butler et al., 2018). The structural interpretation determines the cross-sectional area and final length of section that are two critical parameters in any area balancing. The limited resolution of seismic data causes some inherent uncertainty in structural interpretations, which is often accompanied by unresolved sub-seismic deformation. This is known to be a major source of error in line-length balancing, generally leading to an underestimate of the overall shortening (e.g., Sans et al., 2003; Koyi et al., 2004; Groshong et al., 2012; Allmendinger and Judge, 2013).

Type B

The shape of restored section is a major unknown, which most existing methods treat by simplifying to a sequence of parallel layers or assuming a horizontal regional slope. As outlined in the Background (i.e., The Chamberlin method) and the examples in the Methodology, small changes in the slope of regional can produce significant changes in restored section and in estimated shortening (Fig. 5b). Despite progress of applying various regional slopes to estimate shortening using Model 1, the simplified straight line of original slope is still unlikely to represent the true shape; for example, the shape of sedimentary layers in front of the Hikurangi accretionary prism are not planar, but curved, perhaps in response to flexural loading. So the simplified straight line in theoretical models will produce some errors and uncertainties.

Type C

Layer-parallel strain and lateral compaction are widely recognized in both physical analogue models and natural examples (Koyi et al., 2004; Butler and Paton, 2010; Şengör and Bozkurt, 2013; Lathrop and Burberry, 2017). These are thought to cause a reduction in cross-section area, bed length and volume, that are difficult to assess from current structures. Their contribution to structural shortening remains poorly constrained, as such the shortening quantified by different models will usually be a minimum estimate in thrust systems. Accurate restorations require constraints on magnitude of layer parallel shortening, related layer-perpendicular thickening, and potential area loss.

5.4. Model application

Application of both models requires a certain level of knowledge about the initial wedge geometry. In practice, if the initial surface slope and basal dip are well constrained, using Model 1 to simply restore a deformed wedge to its initial state for shortening estimate would be straightforward. Model 2 needs additional constraint on initial depth to detachment (h_2 in Fig. 4) which is more difficult to obtain, making Model 2 less applicable than Model 1. However, in some cases, if the deformed section has a simple evolution history, and the initial depth to detachment is easy to determine such as the case of scaled physical analogue (Fig. 7), the Model 2 can be easily applied to compute shortening (Fig. 4; equation 16).

This work provides a way of computing shortening for a range of values which is perhaps the more helpful result as opposed to just the shortening estimate. The main learning from this study is that the initial regional slope and basal detachment dip are incredibly important but difficult to constrain. Many previous studies used a single, mostly horizontal, regional slope to compute shortening across a thrust belt based on area balancing may need re-evaluation.

6. Conclusions

In this paper, we developed two new solutions to area balancing of a thrust wedge based on conserved cross-sectional area, assuming an initial trapezium shape. The new methods do not incorporate the usual assumption of a rectangular initial geometry, but instead allow various regional slope and basal dip to be used. They are then tested against scaled physical analogues and natural examples of fold-thrust belt.

A higher regional slope (or basal dip) of the fold-thrust belt results in reduced excess area and therefore reduced estimated shortening, whereas a lower regional slope (or basal dip) leads to increased excess area and thus increased estimated shortening. Because of the difficulty in resolving original wedge taper and observed significance of this geometry, we conclude that the absolute values of shortening are probably not attainable in most thrust belts. Accuracy of shortening estimate requires independent constraint of parameters, particularly the initial regional slope and basal dip, and not just greater precision of the measurements themselves.

The new methods developed and tested here are generally applicable, since they are concerned mainly with gross cross-section area of a system irrespective of lithology, rheology, fluid pressure or other factors that control the form and detailed expression of final structure. The key uncertainties of the new approaches are from structural interpretation, initial wedge shape and penetrative strain. Model 1 is easily applied to compute shortening with known initial surface slope and basal dip while Model 2 requires additional constrain on initial depth to detachment to estimate shortening, which makes it less applicable.

Given the significance of initial wedge taper in area balancing restoration, previous studies used a single, generally horizontal, regional slope to preform area balancing to estimate shortening and/or depth to detachment may need to be revisited.

Acknowledgement

We acknowledge the funding to X. Yang from the UK Natural Environment Research Council (NERC) Centre for Doctoral Training (CDT) in Oil and Gas and the National Oceanography Centre, Southampton and University of Southampton. We very much appreciate the three anonymous reviewers for their robust reviews, insightful comments and important suggestions that significantly improved the manuscript. Line draw seismic profiles are based on seismic data provided by PGS. We thank editor Cara Burberry, Robert Merrill and Frances Whitehurst for handling this paper and providing helpful editorial advice.

Figures

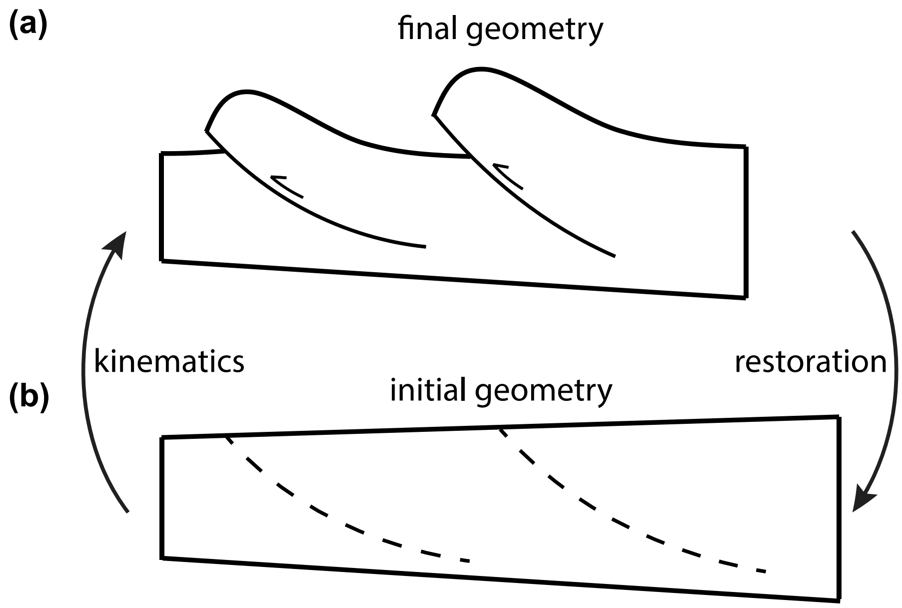

Fig. 1. Schematic diagrams showing the concept of structural restoration. (a) Deformed geological cross-section with known final geometry, (b) restored retro-deformational state of cross-section with predicted initial geometry.

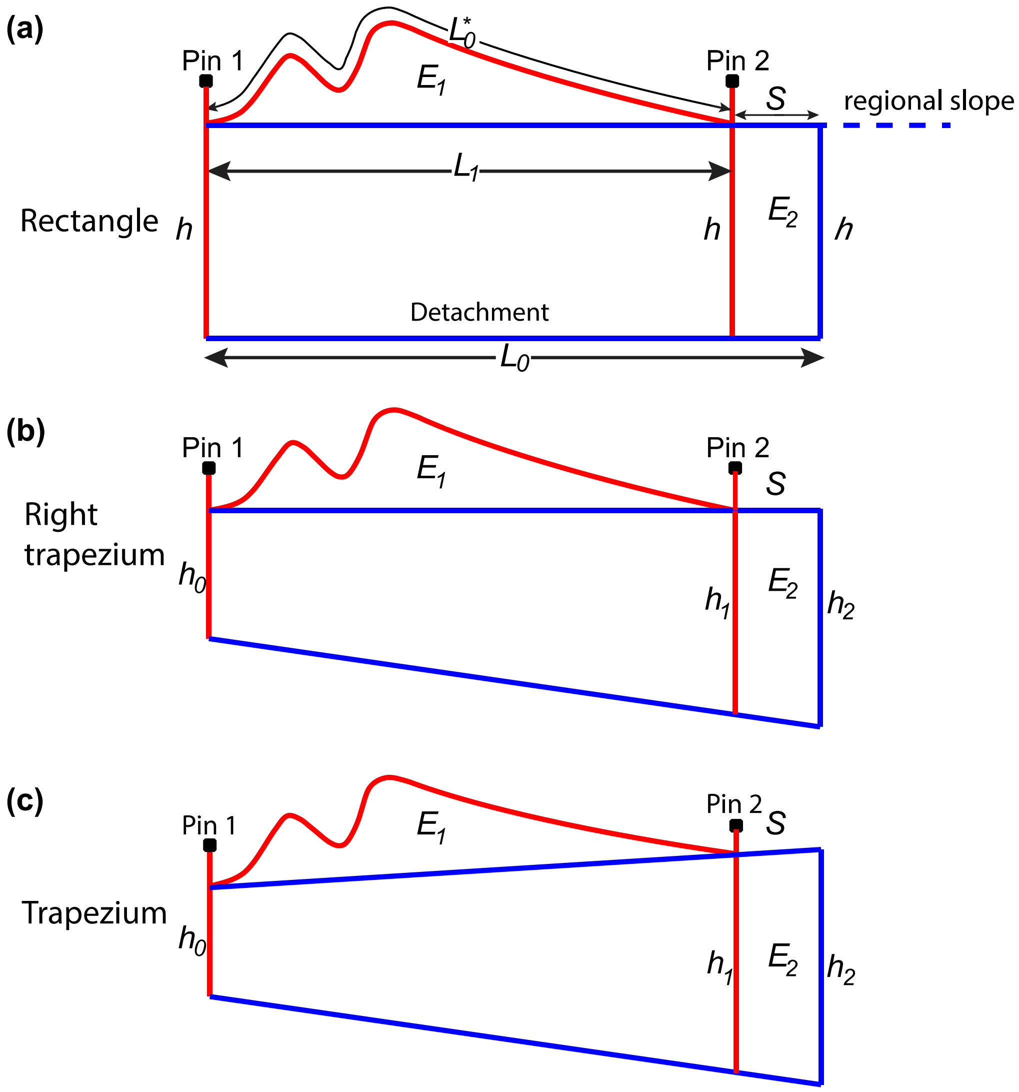

Fig. 2. The relationship between excess area (E_1), shortening above detachment (S), and depth to detachment as formulated by Chamberlin (1910). L_0^* = curved bed length, L_1= length of deformed region, L_0= restored length of cross-section, h and h_0= depth to detachment at the front, h_1= depth to detachment at backstop of deformed section, h_2= depth to detachment at backstop of restored section. (a) Horizontal regional slope and basal detachment; (b) horizontal regional slope and oblique basal detachment; (c) oblique regional slope and basal detachment. The red cross-section represents the final geometry of a deformed thrust wedge, the blue trapeziums are the initial wedge geometry restored based upon different scenarios.

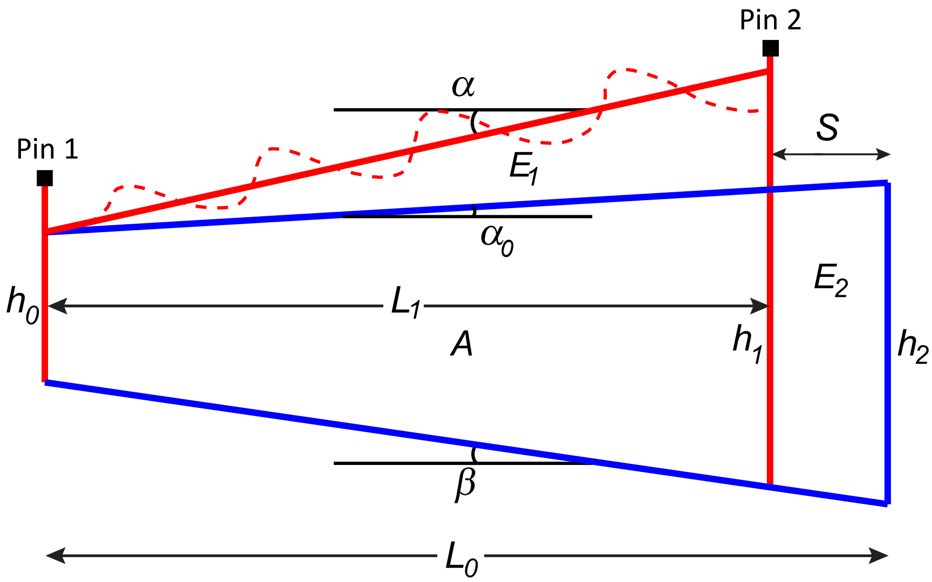

Fig. 3. Model 1. A trapezium model of original (blue) and deformed (red) wedges to show the principles of area balancing restoration, the red dash line represents the topography of a real fold-thrust belt. α= topographic slope, β= basal/detachment dip, α_0= dip of regional slope, E_1= excess area, E_2= displaced area above basal detachment, S= shortening, L_1= length of deformed section, L_0 = length of restored section, H_0= depth to detachment at the fixed pin line, H_1= depth to detachment at the mobile pine line, H_2= depth to detachment at backstop of restored section.

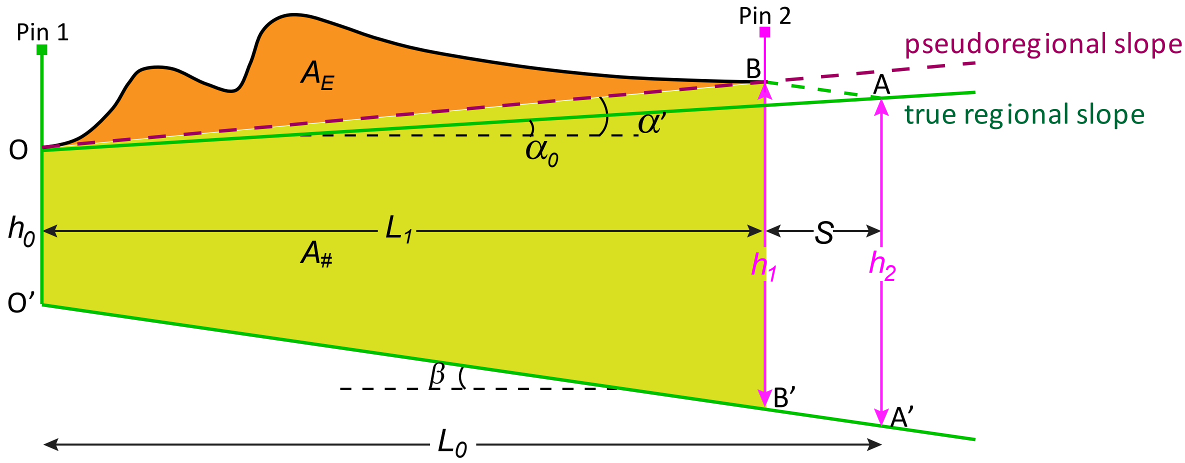

Fig. 4. Model 2. A continuous trapezium model assumes that the material to the right (hinterland) simply moves up the basal detachment with no internal deformation, and that there is continuity between this and the deforming wedge. β= basal dip, α_0 = dip of regional slope, α' = dip of pseudoregional slope, A_E= area above pseudoregional slope, $A_\#$= the below the pseudoregional slope (OBB'O'), S= shortening, L_1= length of deformed section, H_0= depth to detachment at front, H_1= depth to detachment at backstop of deformed section, H_2= depth to detachment at backstop of restored section.

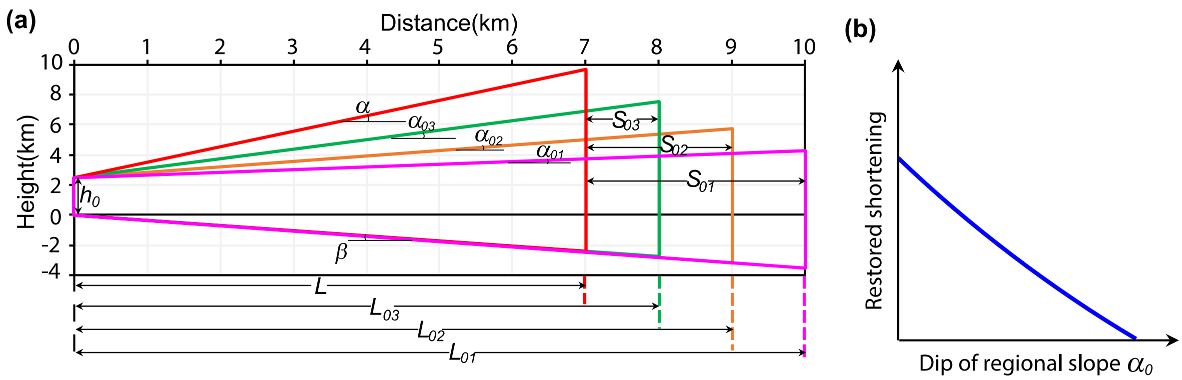

Fig. 5. (a) Example of restoring a simplified thrust belt, i.e., red trapezium using Model 1 with various regional slopes. α_{01}, α_{02} and α_{03} = the assumed regional slope, S_{01}, S_{02} and S_{03} = the calculated shortening, L_{01}, L_{02} and L_{03} = the restored initial length of thrust belt. (b) The predicted linear relationship between restored shortening and dip of regional slope. The green, yellow and pink trapeziums are restored thrust wedge using different regional slopes.

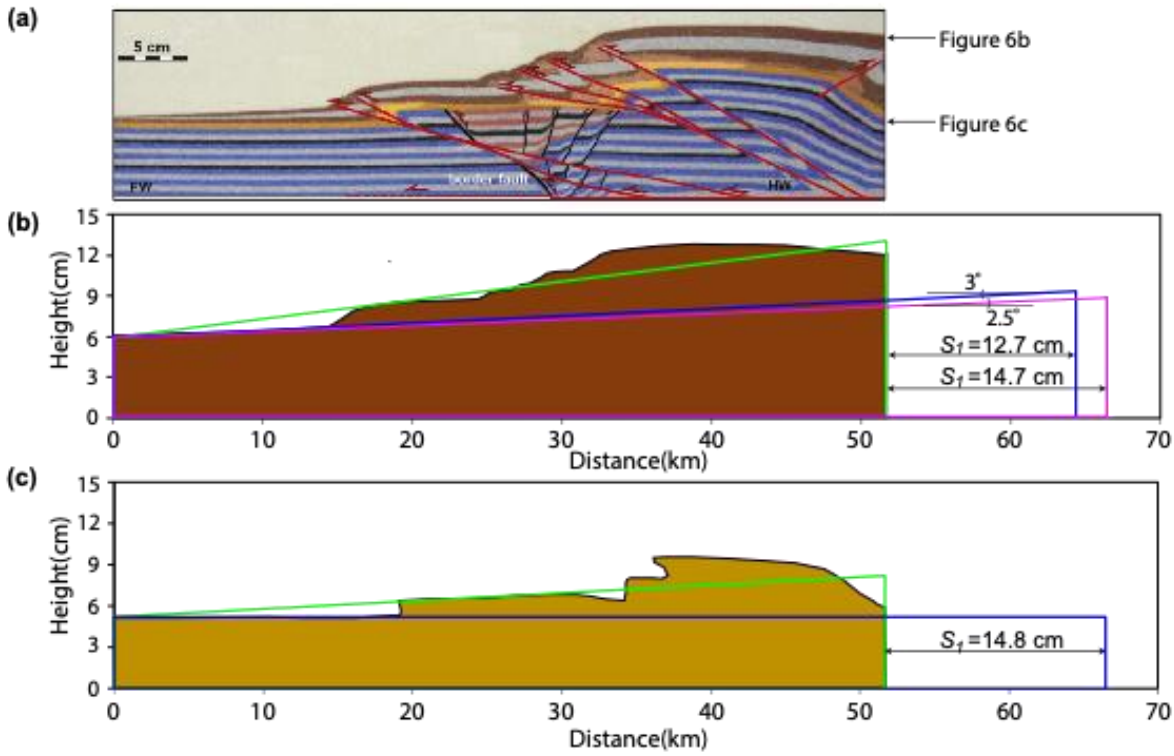

Fig. 6. (a) Example of a sandbox model after 15 cm of shortening, this is the Fig. 11f of Granado et al. (2017). (b) Restoration of the section using Model 1 for the top layer yielding 12.7 cm and 14.7 cm shortening, corresponding to 3° and 2.5° dip of regional slope, respectively. (c) restoration of the section using Model 1 for the horizontal base of yellow layer yielding 14.8 cm shortening. The green trapezium corresponds to the deformed wedge, the blue and pink trapeziums are pre-deformed wedge restored based on different regional slopes.

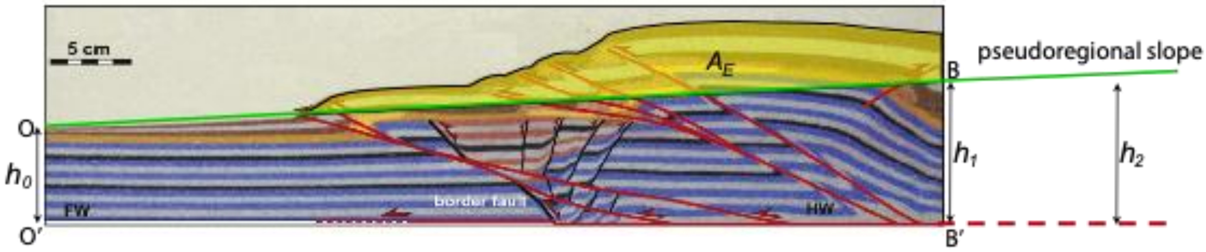

Fig. 7. Restoration of the section using Model 2 for the top layer producing 14.5 cm shortening, the sandbox model is the Fig. 11f of Granado et al. (2017). The transparent yellow area is the area above the pseudoregional slope expressed by the green line.

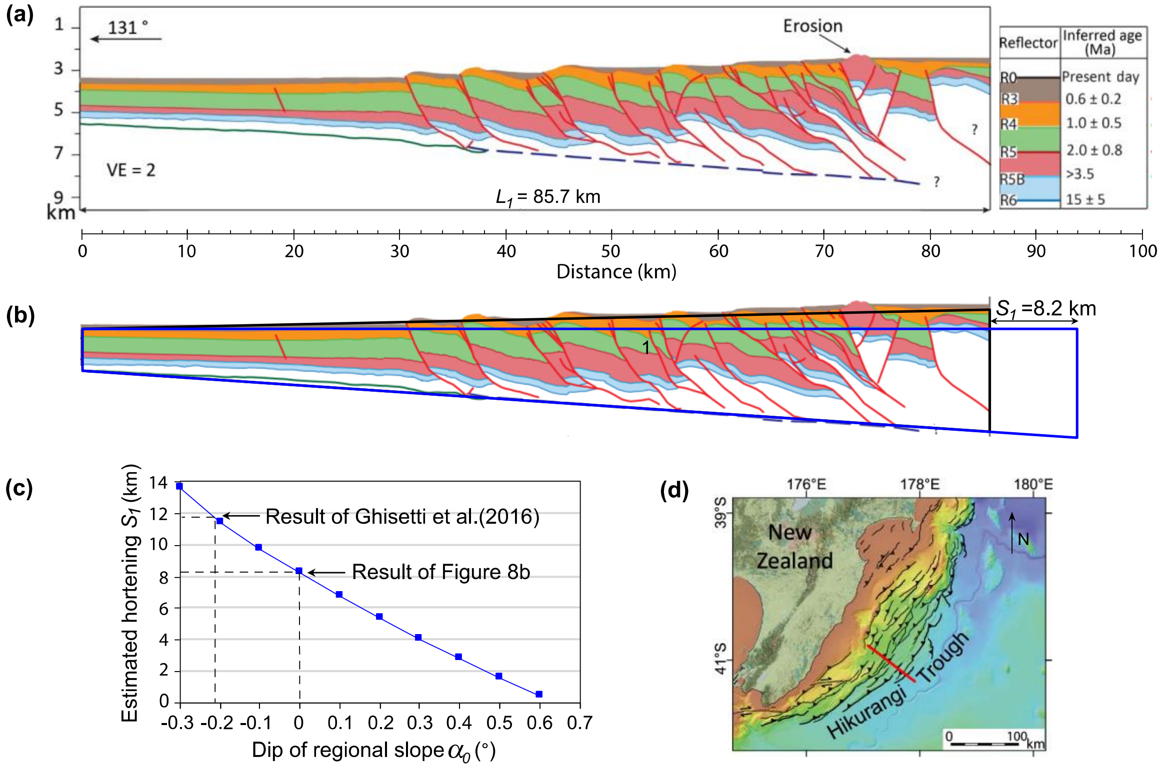

Fig. 8. Restoration of a fold-thrust belt across the Hikurangi accretionary prism, New Zealand. (a) Depth-converted 2D seismic profile with interpreted structure, this is the Transect T03 of Ghisetti et al. (2016). (b) Restored fold-thrust belt (blue trapezium) with a horizontal regional slope yielding 8.2 km of shortening, the black trapezium represents the deformed thrust wedge. (c) Plot of estimated shortening against a range of input dips of regional slope (-0.3° to 0.6°). The dashed line in Fig. 8c shows the result of sequential restoration by Ghisetti et al. (2016) and the result of this study with a horizontal regional slope. (d) The regional map shows the location of seismic profile used in this study, modified from the Fig. 1a of Ghisetti et al. (2016).

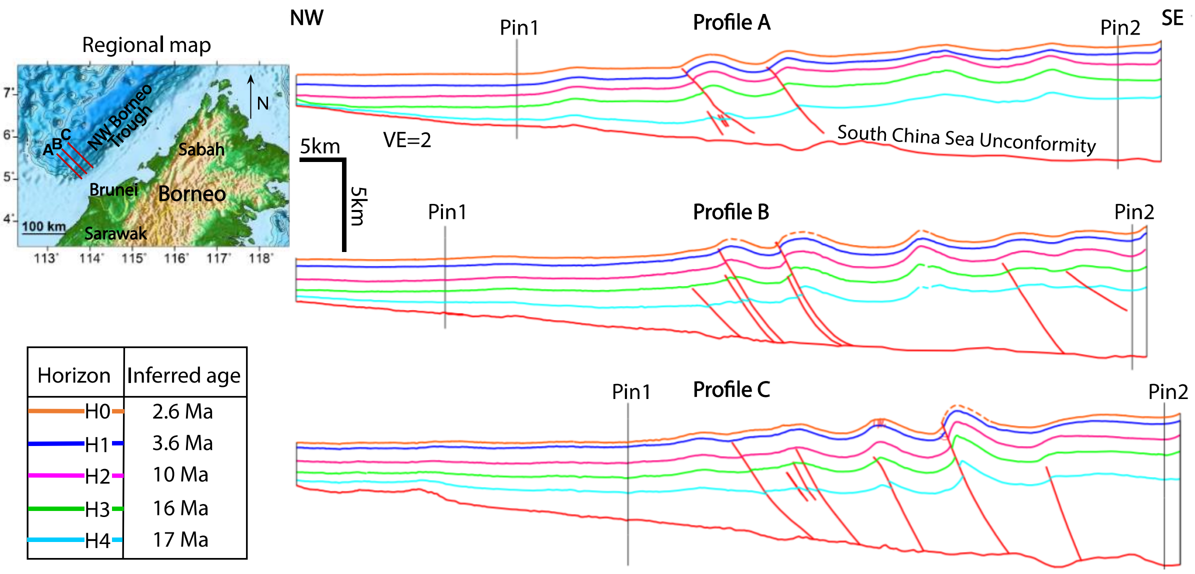

Fig. 9. Fold-thrust belt structures interpreted from 2D depth-converted seismic lines A, B and C (1.5 x vertical exaggeration) across the Brunei portion of the NW Borneo deep water fold-thrust belt, see inset for locations. Five seismic horizons (H0-H4) and a basal detachment (similar position to the South China Sea Unconformity) are mapped from shallow to deep levels. The vertical pine lines define the main deforming region in the thrust belt that is subjected to area balancing restoration. Note the original 2D seismic profiles are not presented here due to the restriction on data publishing.

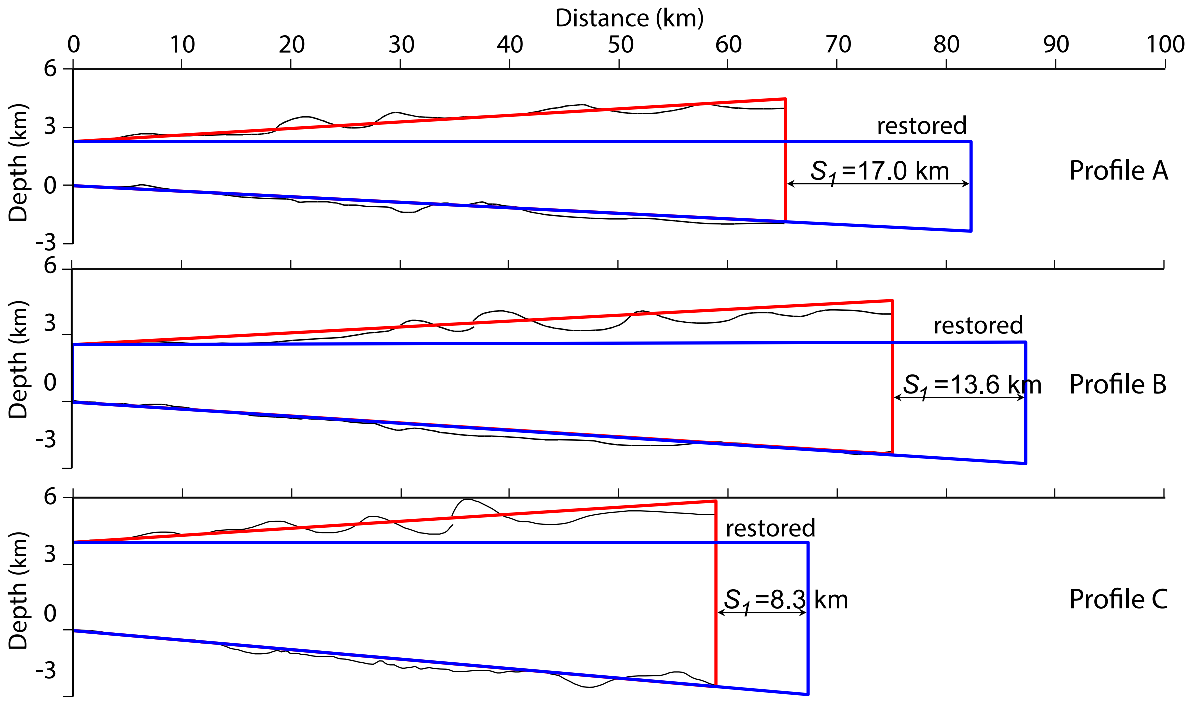

Fig. 10. Structural restoration of the NW Borneo fold-thrust belts enclosed by horizon H1, basal detachment and two pin lines with an arbitrary horizontal regional slope using Model 1. The 17.0 km, 13.6 km and 8.3 km of shortening are estimated for seismic profiles A, B and C, respectively. The black line represents the current geometry of thrust wedge. The red trapeziums are the simplified thrust wedges with same cross-sectional area as the current thrust wedges, the trapeziums are the restored thrust wedges with an assumed horizontal regional dip.

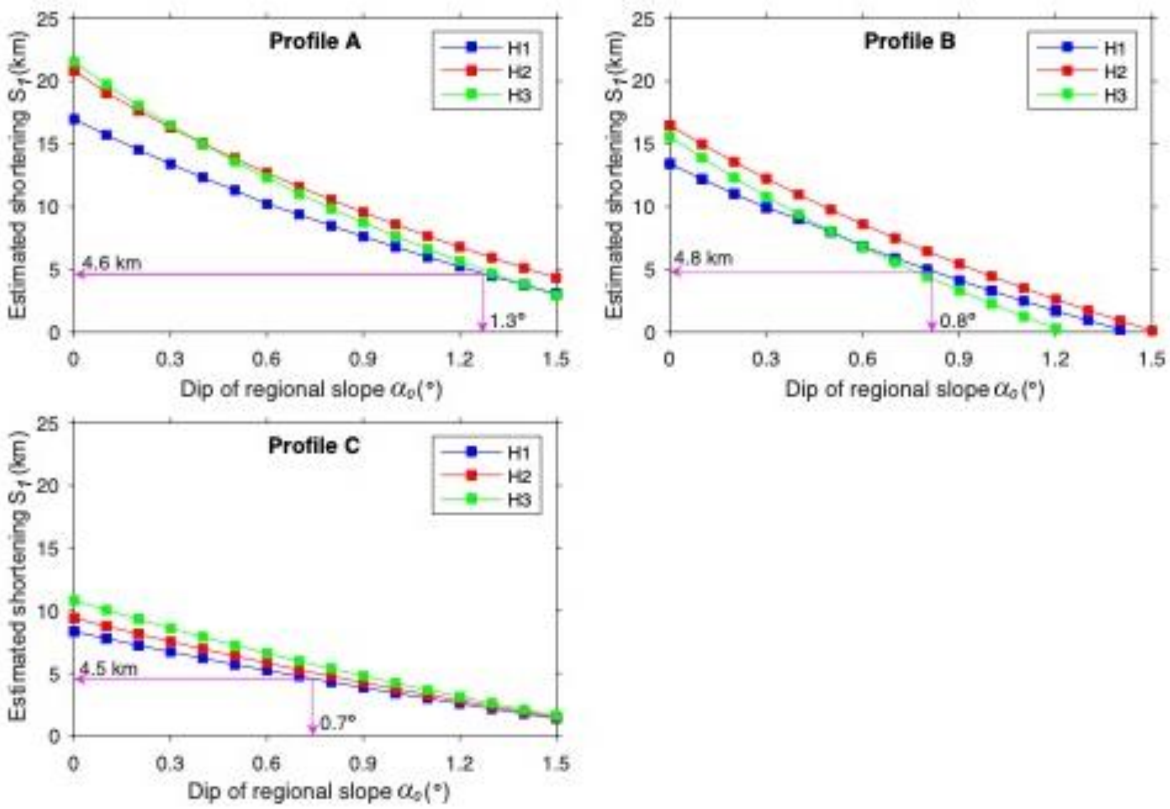

Fig. 11. The results of area balancing restoration for NW Borneo seismic profiles A, B and C with a range of regional dips (0.1-1.5°) using Model 1 for horizons H1-H3 and shortening results obtained with Horizon H1 using Model 2. Note the shortening value predicted using Model 2 is indicated by a pink line, and is then used to constrain the initial regional slope of Horizon 1 for each fold-thrust belt scenario.

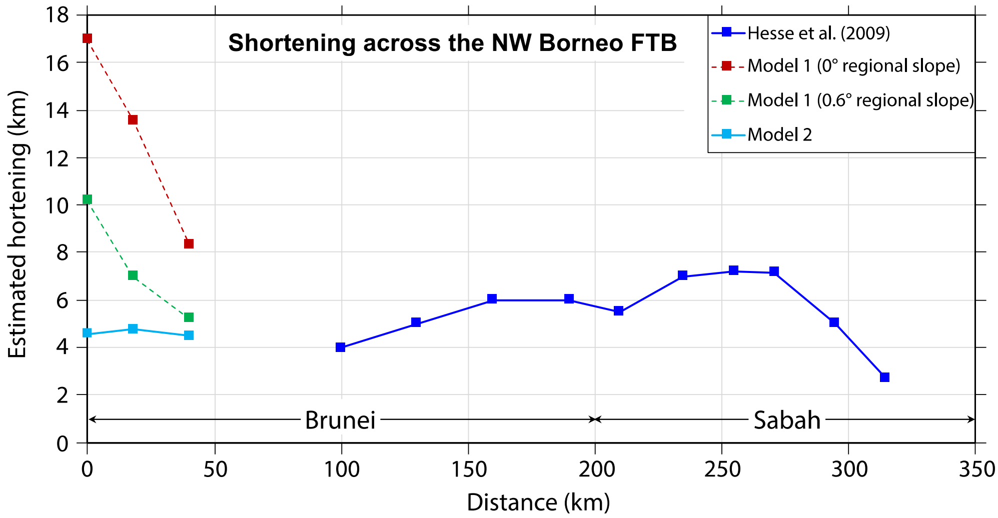

Fig. 12. The along-strike shortening (northeastward) in the NW Borneo fold-thrust belt predicted by this study using Model 1 with 0° and 0.6 ° of regional slopes, and using Model 2, and estimated by Hesse et al. (2009) using sequential restoration. Note this study primarily covers the Southernmost Brunei offshore over a distance of ~40 km whereas the study of Hesse et al. (2009) extends from offshore middle Brunei to offshore Sabah over a much longer distance of 215 km.

Horizon	α_0 (°)	β (°)	L_1 (cm)	H_0 (cm)	H_1 (cm)	H_2 (cm)	A (cm²)	$E_1(E_2)$ (cm²)	A_E (cm²)	$A_\#$ (cm²)	S_1 (cm)	S_2 (cm)	S (cm)
Scaled physical analogue													
Top Brown	3	0	51.7	6.0	8.3	9.1	491.0	128.7	106.8	384.2	12.7	14.5	1.3
	2.5	0	51.7	6.0	8.2	8.7	491.0	107.1			14.7		
Base Yellow	0	0	51.7	5.6	5.6	5.6	375.0	86.7	/	/	14.8	/	7.2
	α_0 (°)	β (°)	L_1 (km)	H_0 (km)	H_1 (km)	H_2 (km)	A (km²)	$E_1(E_2)$ (km²)	A_E (km²)	$A_\#$ (km²)	S_1 (km)	S_2 (km)	S (cm)
Hikurangi Accretionary prism													
R3	0	2.0	85.7	1.9	4.9	5.2	330.7	41.3	/	/	8.2	/	1.2
Seismic profile A													
H1	0	1.4	65.3	2.2	3.8	4.2	280.6	66.8	20.0	260.6	16.7	4.6	1.5
H2	0	1.4	65.3	1.7	3.3	3.8	249.3	73.8	19.5	229.8	20.8	5.4	1.7
H3	0	1.4	65.3	1.0	2.6	3.1	199.4	61.4	18.7	180.7	21.5	6.5	1.6
Seismic profile B													
H1	0	1.9	74.6	2.6	5.1	5.5	350.7	72.1	19.0	331.7	13.6	4.8	0.9
H2	0	1.9	74.6	1.8	4.3	4.8	298.5	75.6	18.2	280.3	16.6	5.3	1.3
H3	0	1.9	74.6	1.2	3.7	4.2	238.8	62.2	16.8	222.0	15.8	6.2	1.0
Seismic profile C													
H1	0	2.5	58.3	4.0	6.5	6.9	360.3	55.8	25.9	330.4	8.3	4.5	1.6
H2	0	2.5	58.3	3.1	5.6	6.1	310.2	55.0	25.3	284.9	9.4	5.1	2.0
H3	0	2.5	58.3	2.3	4.8	5.3	261.5	54.8	24.5	237.0	10.8	5.9	2.1

Table 1. Parameters of fold-thrust belt examples. α_0 = initial regional slope, β=basal dip, L_1 = Length of deformed section, H_0 = depth to detachment at the fixed front, H_1= depth to detachment at the backstop, H_2 = depth to detachment at the restored backstop, A=overall cross-sectional area, E_1 = Area above the regional slope, E_2 = Area displaced above basal detachment, A_E = Area above the pseudoregional slope, $A_\#$ = area below the pseudoregional slope, S_1 = shortening obtained using Model 1, S_2 = shortening obtained using Model 2, S= shortening obtained using bed-length measurement.

References

Allmendinger, R. W., and Judge, P., 2013, Stratigraphic uncertainty and errors in shortening from balanced sections in the North American Cordillera: Geological Society of America Bulletin, v. 125, no. 9-10, p. 1569-1579,doi: 10.1130/B30871.1.

Bally, A. W., Gordy, P. L., and Stewart, G. A., 1966, Structure, seismic data, and orogenic evolution of southern Canadian Rocky Mountains: Canadian Petroleum Geology Bulletin, v. 14, p. 337-381.

Beaumont, C., Fullsack, P., and Hamilton, J., 1992, Erosional control of active compressional orogens, *in* McClay, K. R., ed., Thrust Tectonics: Dordrecht, Springer Netherlands, p. 1-18, doi: 10.1007/978-94-011-3066-0_1

Beck, C., Deville, E., Blanc, E., Philippe, Y., and Tardy, M., 1998, Horizontal shortening control of Middle Miocene marine siliciclastic accumulation (Upper Marine Molasse) in the southern termination of the Savoy Molasse Basin (northwestern Alps/southern Jura): Geological Society, London, Special Publications, v. 134, no. 1, p. 263-278,doi: 10.1144/GSL.SP.1998.134.01.12.

Bond, C. E., 2015, Uncertainty in structural interpretation: Lessons to be learnt: Journal of Structural Geology, v. 74, p. 185-200, doi:10.1016/j.jsg.2015.03.003.

Boyer, S. E., 1995, Sedimentary basin taper as a factor controlling the geometry and advance of thrust belts: American Journal of Science, v. 295, no. 10, p. 1220-1254, doi: 10.2475/ajs.295.10.1220.

Boyer, S. E., and Elliott, D., 1982, Thrust systems: AAPG Bulletin, v. 66, no. 9, p. 1196-1230.

Bucher, W. H., 1933, The deformation of the earth's crust: Princeton, Princeton University Press, 518p.

Buiter, S. J., Schreurs, G., Albertz, M., Gerya, T. V., Kaus, B., Landry, W., Le Pourhiet, L., Mishin, Y., Egholm, D. L., and Cooke, M., 2016, Benchmarking numerical models of brittle thrust wedges: Journal of structural geology, v. 92, p. 140-177,doi: 10.1016/j.jsg.2016.03.003.

Bulnes, M., and Poblet, J., 1999, Estimating the detachment depth in cross sections involving detachment folds: Geological Magazine, v. 136, no. 4, p. 395-412, doi:10.1017/S0016756899002794.

Butler, R., Mazzoli, S., Corrado, S., De Donatis, M., Di Bucci, D., Gambini, R., Naso, G., Nicolai, C., Scrocca, D., and Shiner, P., 2004, Applying thick-skinned tectonic models to the Apennine thrust belt of Italy—Limitations and implications, *in* McClay, K.R., ed., Thrust tectonics and hydrocarbon systems: AAPG Memoir 82, p. 647-667.

Butler, R., and Paton, D., 2010, Evaluating lateral compaction in deepwater fold and thrust belts: How much are we missing from “nature’s sandbox”: GSA Today, v. 20, no. 3, p. 4-10, doi: 10.1130/GSATG77A.1.

Butler, R. W., Bond, C. E., Cooper, M. A., and Watkins, H., 2018, Interpreting structural geometry in fold-thrust belts: Why style matters: Journal of Structural Geology, v. 114, p. 251-273, doi: 10.1016/j.jsg.2018.06.019.

Butler, R. W. H., 2013, Area balancing as a test of models for the deep structure of mountain belts, with specific reference to the Alps: Journal of Structural Geology, v. 52, p. 2-16, doi: 10.1016/j.jsg.2013.03.009.

Chamberlin, R. T., 1910, The Appalachian folds of central Pennsylvania: The Journal of Geology, v. 18, no. 3, p. 228-251.

Corredor, F., Shaw, J. H., and Bilotti, F., 2005, Structural styles in the deep-water fold and thrust belts of the Niger Delta: AAPG Bulletin, v. 89, no. 6, p. 753-780, doi: 10.1306/02170504074.

Cruz, L., Malinski, J., Wilson, A., Take, W., and Hilley, G., 2010, Erosional control of the kinematics and geometry of fold-and-thrust belts imaged in a physical and numerical sandbox: Journal of Geophysical Research: Solid Earth, v. 115, no. B09404, doi: 10.1029/2010JB007472.

Dahlen, F. A., 1990, Critical taper model of fold-and-thrust belts and accretionary wedges: Annual Review of Earth and Planetary Sciences, v. 18, p. 55-99, doi: 10.1146/annurev.ea.18.050190.000415.

Dahlstrom, C., 1969, Balanced cross sections: Canadian Journal of Earth Sciences, v. 6, no. 4, p. 743-757.

Dahlstrom, C. D. A., 1990, Geometric Constraints Derived from the Law of Conservation of Volume and Applied to Evolutionary Models for Detachment Folding: AAPG Bulletin, v. 74, no. 3, p. 336-344.

Davis, D., Suppe, J., and Dahlen, F. A., 1983, Mechanics of fold-and-thrust belts and accretionary wedges: Journal of Geophysical Research, v. 88, no. B2, p. 1153-1172, doi: 10.1029/JB088iB02p01153.

DeCelles, P. G., Gehrels, G. E., Quade, J., Ojha, T. P., Kapp, P. A., and Upreti, B. N., 1998, Neogene foreland basin deposits, erosional unroofing, and the kinematic history of the Himalayan fold-thrust belt, western Nepal: Geological Society of America Bulletin, v. 110, no. 1, p. 2-21, doi: 10.1130/0016-7606(1998)110<0002:NFBDEU>2.3.CO;2.

Epard, J. L., and Groshong, R. H., 1993, Excess Area and Depth to Detachment: AAPG Bulletin, v. 77, no. 8, p. 1291-1302.

Epard, J. L., and Groshong, R. H., 1995, Kinematic model of detachment folding including limb rotation, fixed hinges and layer-parallel strain: Tectonophysics, v. 247, no. 1-4, p. 85-103, doi: 10.1016/0040-1951(94)00266-C.

Faill, R. T., and Nickelsen, R. P., 1999, Appalachian Mountain section of the Ridge and Valley province, *in* Schultz, C.H., ed., The Geology of Pennsylvania: Geological Survey of Pennsylvania Special Publication, v. 1, no. 269-285.

Fillon, C., Huismans, R. S., and van der Beek, P., 2013, Syntectonic sedimentation effects on the growth of fold-and-thrust belts: Geology, v. 41, no. 1, p. 83-86, doi: 10.1130/G33531.1.

Fitz-Diaz, E., Hudleston, P., and Tolson, G., 2011, Comparison of tectonic styles in the Mexican and Canadian Rocky Mountain Fold-Thrust Belt, in Poblet, J., and Lisle, R. J., eds., Kinematic Evolution and Structural Styles of Fold-and-Thrust Belts, v.349, p. 149-167.

Fossen, H., 2016, Structural Geology: Cambridge, Cambridge University Press, 524p.

Gee, M. J. R., Uy, H. S., Warren, J., Morley, C. K., and Lambiase, J. J., 2007, The Brunei slide: A giant submarine landslide on the North West Borneo Margin revealed by 3D seismic data: Marine Geology, v. 246, no. 1, p. 9-23, doi: 10.1016/j.margeo.2007.07.009.

Ghisetti, F. C., Barnes, P. M., Ellis, S., Plaza-Faverola, A. A., and Barker, D. H., 2016, The last 2 Myr of accretionary wedge construction in the central Hikurangi margin (North Island, New Zealand): Insights from structural modeling: Geochemistry, Geophysics, Geosystems, v. 17, no. 7, p. 2661-2686, doi:10.1002/2016GC006341.

Goguel, J., 1962, Tectonics: San Francisco, Freeman, 384p.

Granado, P., Ferrer, O., Muñoz, J., Thöny, W., and Strauss, P., 2017, Basin inversion in tectonic wedges: Insights from analogue modelling and the Alpine-Carpathian fold-and-thrust belt: Tectonophysics, v. 703, p. 50-68, doi: 10.1016/j.tecto.2017.02.022.

Groshong Jr, R. H., 2019, Area-constant strain and dilation in sandbox models: Insights from whole-model area balance: Journal of Structural Geology, v. 118, p. 279-283, doi: 10.1016/j.jsg.2018.11.003.

Groshong, R. H., and Epard, J. L., 1994, The role of strain in area-constant detachement folding: Journal of Structural Geology, v. 16, no. 5, p. 613-618, doi: 10.1016/0191-8141(94)90113-9.

Groshong, R. H., Withjack, M. O., Schlische, R. W., and Hidayah, T. N., 2012, Bed length does not remain constant during deformation: Recognition and why it matters: Journal of Structural Geology, v. 41, p. 86-97, doi: 10.1016/j.jsg.2012.02.009.

Hesse, S., Back, S., and Franke, D., 2009, The deep-water fold-and-thrust belt offshore NW Borneo: Gravity-driven versus basement-driven shortening: Geological Society of America Bulletin, v. 121, no. 5-6, p. 939-953, doi: 10.1130/B26411.1.

Hesse, S., Back, S., and Franke, D., 2010, The structural evolution of folds in a deepwate fold and thrust belt - a case study from the Sabah continental margin offshore NW Borneo, SE Asia: Marine and Petroleum Geology, v. 27, p. 442-454, doi: 10.1016/j.marpetgeo.2009.09.004.

Hilley, G., and Strecker, M. R., 2004, Steady state erosion of critical Coulomb wedges with applications to Taiwan and the Himalaya: Journal of Geophysical Research: Solid Earth, v. 109, no. B01411, doi:10.1029/2002JB002284.

Hinz, K., Fritsch, J., Kempter, E. H. K., Mohammad, A. M., Meyer, J., Mohamed, D., Vosberg, H., Weber, J., and Benavidez, J., 1989, Thrust tectonics along the north-western continental margin of Sabah/Borneo: Geologische Rundschau, v. 78, no. 3, p. 705-730.

Hinz, K., and Schluter, H. U., 1985, Geology of the Dangerous Grounds, South China Sea, and the Continental Margin off Southwest Palawan: Results of SONNE cruises SO-23 and SO-27: Energy, v. 10, no. 3-4, p. 297-315.

Hossack, J. R., 1979, The use of balanced cross-sections in the calculation of orogenic contraction: A review: Journal of the Geological Society, v. 136, no. 6, p. 705-711, doi: 10.1144/gsjgs.136.6.0705.

Hoth, S., Hoffmann-Rothe, A., and Kukowski, N., 2007, Frontal accretion: An internal clock for bivergent wedge deformation and surface uplift: Journal of Geophysical Research: Solid Earth, v. 112, no. B06408, doi:10.1029/2006JB004357.

Hubbard, J., Almeida, R., Foster, A., Sapkota, S. N., Bürgi, P., and Tapponnier, P., 2016, Structural segmentation controlled the 2015 Mw 7.8 Gorkha earthquake rupture in Nepal: Geology, v. 44, no. 8, p. 639-642, doi: 10.1130/G38077.1.

Ingram, G. M., Chisholm, T. J., Grant, C. J., Hedlund, C. A., Stuart-Smith, P., and Teasdale, J., 2004, Deepwater North West Borneo: Hydrocarbon accumulation in an active fold and thrust belt: Marine and Petroleum Geology, v. 21, no. 7, p. 879-887, doi: 10.1016/j.marpetgeo.2003.12.007.

Judge, P. A., and Allmendinger, R. W., 2011, Assessing uncertainties in balanced cross sections: Journal of Structural Geology, v. 33, no. 4, p. 458-467, doi: 10.1016/j.jsg.2011.01.006.

Koyi, H. A., Sans, M., Teixell, A., Cotton, J., and Zeyen, H., 2004, The significance of penetrative strain in the restoration of shortened layers—insights from sand models and the Spanish Pyrenees, *in* McClay, K.R., ed., Thrust tectonics and hydrocarbon systems: AAPG Memoir 82, p. 1-16.

Lathrop, B. A., and Burberry, C. M., 2017, Accommodation of penetrative strain during deformation above a ductile decollement: Lithosphere, v. 9, no. 1, p. 46-57, doi: 10.1130/L558.1.

Lickorish, W. H., and Ford, M., 1998, Sequential restoration of the external Alpine Digne thrust system, SE France, constrained by kinematic data and synorogenic sediments: Geological Society, London, Special Publications, v. 134, no. 1, p. 189-211, doi: 10.1144/GSL.SP.1998.134.01.09.

Masini, M., Bigi, S., Poblet, J., Bulnes, M., Di Cuia, R., and Casabianca, D., 2011, Kinematic evolution and strain simulation, based on cross-section restoration, of the Maiella Mountain: an analogue for oil fields in the Apennines (Italy), in Poblet, J., and Lisle, R. J., eds., Kinematic Evolution and Structural Styles of Fold-and-Thrust Belts, v. 349, p. 25-44, doi: https://doi.org/10.1144/SP349.2.

McQuarrie, N., 2002, The kinematic history of the central Andean fold-thrust belt, Bolivia: Implications for building a high plateau: Geological Society of America Bulletin, v. 114, no. 8, p. 950-963, doi: 10.1130/0016-7606(2002)114<0950:TKHOTC>2.0.CO;2.

McQuarrie, N., 2004, Crustal scale geometry of the Zagros fold-thrust belt, Iran: Journal of Structural Geology, v. 26, no. 3, p. 519-535, doi: 10.1016/j.jsg.2003.08.009.

Mishra, P., and Mukhopadhyay, D. K., 2012, Structural evolution of the frontal fold–thrust belt, NW Himalayas from sequential restoration of balanced cross-sections and its hydrocarbon potential: Geological Society, London, Special Publications, v. 366, p. 201-228, doi: 10.1144/SP366.6.

Mitra, G., 1997, Evolution of salients in a fold-and-thrust belt: The effects of sedimentary basin geometry, strain distribution and critical taper, *in* Sengupta, S., ed., Evolution of geological structures in micro-to macro-scales: London, Chapman & Hall, p. 59-90.

Mitra, S., and Namson, J., 1989, Equal-area balancing: American Journal of Science, v. 289, no. 5, p. 563-599, doi: 10.2475/AJS.289.5.563.

Molinaro, M., Leturmy, P., Guezou, J. C., Frizon de Lamotte, D., and Eshraghi, S., 2005, The structure and kinematics of the southeastern Zagros fold-thrust belt, Iran: From thin-skinned to thick-skinned tectonics: Tectonics, v. 24, no. TC3007, doi: 10.1029/2004TC001633.

Moretti, I., and Callot, J. P., 2012, Area, length and thickness conservation: Dogma or reality?: Journal of Structural Geology, v. 41, p. 64-75, doi: 10.1016/j.jsg.2012.02.014.

Moretti, I., Delos, V., Letouzey, J., Otero, A., and Calvo, J., 2007, The use of surface restoration in foothills exploration: theory and application to the Sub-Andean Zone of Bolivia, in Lacombe, O., Lavé J., Roure, F., Vergés, J., ed., Thrust Belts and Foreland Basins. Frontiers in Earth Sciences: Berlin, Springer, p. 149-162, doi: 10.1007/978-3-540-69426-7_8.

Moretti, I., Letouzey, J., Otero, A., and Calvo, J., 2006, Structures Growing And Decollement Level Role In The Sub Andean Zone Of Bolivia.Caipipendi Block: EAGE Conference proceedings, 9th Simposio Bolivariano - Exploracion Petrolera en las Cuencas Subandinas, doi: 10.3997/2214-4609-pdb.111.15.

Morley, C. K., 2007a, Interaction between critical wedge geometry and sediment supply in a deep-water fold belt: Geology, v. 35, no. 2, p. 139-142, doi: 10.1130/G22921A.1.

Morley, C. K., 2007b, Development of crestal normal faults associated with deepwater fold growth: Journal of Structural Geology, v. 29, no. 7, p. 1148-1163, doi: 10.1016/j.jsg.2007.03.016.

Morley, C.K., 2009a, Geometry of an oblique thrust fault zone in deepwater fold beld from 3D seismic data: Journal of Structural Geology, v. 31, p. 1540-1555, doi: 10.1016/j.jsg.2009.08.015.

Morley, C. K., 2009b, Growth of folds in a deep-water setting: Geosphere, v. 5, no. 2, p. 59-89, doi: 10.1130/GES00186.1.

Morley, C. K., Tingay, M., Hillis, R., and King, R., 2008, Relationship between structural style, overpressures, and modern stress, Baram Delta Province, northwest Borneo: Journal of Geophysical Research-Solid Earth, v. 113, no. B09410, doi: 10.1029/2007JB005324.

Ramsay, J. G., and Huber, M. I., 1987, The techniques of modern structural geology: Cambridge, MA, Academic Press, 391p.

Sans, M., Vergés, J., Gomis, E., Parés, J., Schiattarella, M., Travé, A., Calvet, F., Santanach, P., and Doulcet, A., 2003, Layer parallel shortening in salt-detached folds: constraint on cross-section restoration: Tectonophysics, v. 372, no. 1, p. 85-104,doi: 10.1016/S0040-1951(03)00233-6.

Schlische, R. W., Groshong, R. H., Withjack, M. O., and Hidayah, T. N., 2014, Quantifying the geometry, displacements, and subresolution deformation in thrust-ramp anticlines with growth and erosion: From models to seismic-reflection profile: Journal of Structural Geology, v. 69, p. 304-319, doi: 10.1016/j.jsg.2014.07.012.

Schori, M., Mosar, J., and Schreurs, G., 2015, Multiple detachments during thin-skinned deformation of the Swiss Central Jura: a kinematic model across the Chasseral: Swiss journal of geosciences, v. 108, no. 2-3, p. 327-343, doi: 10.1007/s00015-015-0196-x.

Schreurs, G., Buiter, S. J., Boutelier, J., Burberry, C., Callot, J.-P., Cavozzi, C., Cerca, M., Chen, J.-H., Cristallini, E., and Cruden, A. R., 2016, Benchmarking analogue models of brittle thrust wedges: Journal of structural geology, v. 92, p. 116-139,doi: 10.1016/j.jsg.2016.03.005.

Schreurs, G., Buiter, S. J. H., Boutelier, D., Corti, G., Costa, E., Cruden, A. R., Daniel, J.-M., Hoth, S., Koyi, H. A., Kukowski, N., Lohrmann, J., Ravaglia, A., Schlische, R. W., Withjack, M. O., Yamada, Y., Cavozzi, C., Del Ventisette, C., Brady, J. A. E., Hoffmann-Rothe, A., Mengus, J.-M., Montanari, D., and Nilforoushan, F., 2006, Analogue benchmarks of shortening and extension experiments, in Buiter, S. J. H., and Schreurs, G., eds., Analogue and Numerical Modelling of Crustal-Scale Processes, v. 253, p. 1-27, doi: 10.1144/GSL.SP.2006.253.01.01.

Şengör, A. C., and Bozkurt, E., 2013, Layer-parallel shortening and related structures in zones undergoing active regional horizontal extension: International Journal of Earth Sciences, v. 102, no. 1, p. 101-119, doi: 10.1007/s00531-012-0777-0.

Storti, F., and McClay, K., 1995, Influence of syntectonic sedimentation on thrust wedges in analogue models: Geology, v. 23, no. 11, p. 999-1002, doi: 10.1130/0091-7613(1995)023<0999:IOSSOT>2.3.CO;2.

Totake, Y., Butler, R. W. H., Bond, C. E., and Aziz, A., 2018, Analyzing structural variations along strike in a deep-water thrust belt: Journal of Structural Geology, v. 108, p. 213-229, doi: 10.1016/j.jsg.2017.06.007.

Wang, W., Yin, H., Jia, D., Wu, Z., Wu, C., and Zhou, P., 2018, Calculating detachment depth and dip angle in sedimentary wedges using the area–depth graph: Journal of Structural Geology, v. 107, p. 1-11, doi: 10.1016/j.jsg.2017.11.014.

Wilkerson, M. S., and Dicken, C. L., 2001, Quick-look techniques for evaluating twodimensional cross sections in detached contractional settings: AAPG Bulletin, v. 85, p. 1759-1770, doi: 10.1306/8626D063-173B-11D7-8645000102C1865D.

Willett, S. D., 1999, Orogeny and orography: The effects of erosion on the structure of mountain belts: Journal of Geophysical Research: Solid Earth, v. 104, no. B12, p. 28957-28981, doi: 10.1029/1999JB900248.

Wiltschko, D. V., and Groshong, R. H., 2012, The Chamberlin 1910 balanced section: Context, contribution, and critical reassessment: Journal of Structural Geology, v. 41, p. 7-23, doi: 10.1016/j.jsg.2012.01.019.

Woodward, N. B., Boyer, S. E., and Suppe, J., 1990, Balanced Geological Cross-Sections: Balanced Geological Cross-Sections: An Essential Technique in Geological Research and Exploration: American Geophysical Union, v. 6, p. 1-126, doi: 10.1029/SC006.

Wu, J. E., and McClay, K. R., 2011, Two-dimensional Analog Modeling of Fold and Thrust Belts : Dynamic Interactions with Syncontractional Sedimentation and Erosion, in McClay, K. R., Shaw, J. H., and Suppe, J., eds., Thrust fault-related folding, AAPG Memoir 94, p. 301-333, doi: 10.1306/13251343M9450.

Yin, A., and Kelty, T. K., 1991, Structural Evolution of the Lewis Plate in Glacier-National-Park, Montana - Implications for Regional Tectonic Development: Geological Society of America Bulletin, v. 103, no. 8, p. 1073-1089, doi: 10.1130/00167606(1991)103<1073:SEOTLP>2.3.CO;2.

Yin, H., and R. H. Groshong, Jr., 2006, Balancing and restoration of piercement structures: Geologic insights from 3D kinematicmodels: Journal of Structural Geology, v. 29, p. 99– 114, doi: 10.1016/j.jsg.2005.09.005.

Xiaodong Yang is a professor of Xiaodong Yang is a professor of marine tectonics at South China Sea Institute of Oceanology, Chinese Academy of Sciences. He received his PhD in Structural Geology and Tectonics from University of Southampton. Yang's main research interests include active tectonics, earthquake geology, mechanics of fold-thrust belts, structural restoration methods, tectonic deformation and geohazards in convergent margins.

David Sanderson is Emeritus Professor of Tectonics and Geomechanics at the University of Southampton. His main research interests are faulting, fracturing, and fluid flow, with applications in the hydrocarbon, mineral, and engineering industries. He has published over 170 scientific articles and a book on distinct element modeling of deformation and fluid flow in fractured rock.

Lisa McNeill is a Professor of Tectonics at the University of Southampton. She received a PhD from Oregon State University and then held a Royal Society Dorothy Hodgkin Fellowship at the University of Leeds. McNeill’s research focuses on the active tectonics and geohazards of subduction zones and rift zones. She was recently awarded the Geological Society of London’s Coke Medal.

Frank J. Peel's research interests include salt tectonics, gravity-driven deformation, fluid flow and exploration risk. He is a recipient of the AAPG’s Matson Award. He received his doctoral degree from the University of Oxford. From 1985 to 2013, he worked in the petroleum industry as a senior geoscience advisor and structural geologist at BP and BHP. His current research focusses on salt tectonics at AGL, the University of Texas at Austin.